

Article

Variable Power Tracking Control Strategy of Doubly Fed Induction Generators for Fast Frequency Responses

Xiaocen Xue , Jiejie Huang  and Shun Sang *

School of Electric Engineering, Nantong University, Nantong 226010, China; xiaocenzue@ntu.edu.cn (X.X.); huangjiejie@ntu.edu.cn (J.H.)

* Correspondence: shunsang@ntu.edu.cn

Abstract: Frequency regulation and droop control of doubly fed induction generators (DFIGs) can quickly respond to frequency changes and reduce the maximum rate of frequency (MROFF) in power systems. However, due to real-time dynamic changes in the MPPT control loop, the ability to improve the lowest frequency point is limited. Therefore, this article first describes an in-depth analysis of the dynamic characteristics of the incremental power of frequency regulation with droop control using an equivalent linear model. The limitations of improving the lowest frequency point under the influence of dynamic changes in the MPPT control loop are revealed. Secondly, to address the impact of these dynamics, an improved decoupling frequency regulation (IDFR) strategy based on power tracking is proposed, aiming to increase the maximum frequency deviation (MFD) and MROCOF. Then, in order to overcome the difficulty of adjusting control coefficients in the IDFR strategy, an adaptive control coefficient tuning fuzzy control method based on frequency deviation and ROCOF was proposed to flexibly adjust control requirements under various working conditions, thereby improving the control stability and performance of the system and effectively solving the problem of control coefficient allocation. Finally, to verify the frequency regulation performance of the proposed IDFR strategy under various operating conditions, simulations were conducted based on different disturbances and wind conditions. The results show that the proposed IDFR strategy significantly improves the system MFD and MROCOF improvement ability under various conditions.

Keywords: frequency regulation control; droop control; equivalent linear model; DFIG; improved decoupling frequency regulation



Citation: Xue, X.; Huang, J.; Sang, S. Variable Power Tracking Control Strategy of Doubly Fed Induction Generators for Fast Frequency Responses. *Electronics* **2024**, *13*, 1071. <https://doi.org/10.3390/electronics13061071>

Academic Editor: Davide Astolfi

Received: 24 January 2024

Revised: 1 March 2024

Accepted: 11 March 2024

Published: 14 March 2024



Copyright: © 2024 by the authors. Licensee MDPI, Basel, Switzerland. This article is an open access article distributed under the terms and conditions of the Creative Commons Attribution (CC BY) license (<https://creativecommons.org/licenses/by/4.0/>).

1. Introduction

With the rapid growth of the wind power industry, DFIGs are gradually replacing traditional synchronous generators (TSGs) and connecting to the power grid, leading to an evolution of the power grid structure [1]. However, under this new power grid structure, DFIGs cannot achieve instant matching with frequency due to their special structure, and therefore cannot actively adapt to changes in frequency, which affects the overall inertia and frequency response ability of the grid [2,3]. Especially in high-wind-penetrated grids, DFIGs may be more prone to triggering frequency load shedding protection, posing a threat to the safe and stable operation of the power grid [4].

As in [5], the rotors of DFIGs have significant frequency regulation (FR) potential due to their wide operating range, and compared to TSG, DFIGs may improve their FR per megawatt by several times. This has attracted widespread attention from many power system operators and countries, including China, Eir Grid, the National Grid of the UK, etc., which have all formulated specific requirements for FR and the inertia control of DFIGs, enabling wind-power-connected power systems to meet certain standards and performance levels in FR and inertia [6–10].

Inertial control is a key technology in power system FR control. Its main goal is to improve the frequency change rate (df/dt) of the system, so as to realize the inertial response

of the DFIG controlled by the converter to the power grid [11]. The droop control of DFIGs aims to suppress the frequency drop by establishing a coupling relationship between frequency offset and wind turbine droop characteristics [12]. Through droop control, the system can more effectively respond to external disturbances and maintain frequencies within the allowable range. Ref. [13] proposed a method for evaluating FR capability by comprehensively considering indicators that provide inertia and main frequency support, which helped to provide a more comprehensive understanding of the performance of droop control. In addition, the droop control coefficient plays a crucial role in FR, and its fixed parameters limit the adaptability of DFIGs in the face of different disturbances and operating conditions [14]. To address this issue, an innovative adaptive frequency control strategy is proposed which takes into account factors such as rotor speed, released kinetic energy, and system frequency dynamics and adapts frequency adjustments to different operating conditions by adjusting control coefficients [15–17]. However, the decrease in rotor speed under this adaptive frequency control strategy may lead to DFIGs deviating from the MPPT operation, and this phenomenon will become more pronounced as the control coefficient increases, thereby reducing the additional FR power injected by DFIGs into the grid. In order to ensure a balance between MPPT and frequency regulation in the system, it is necessary to conduct more in-depth research and optimization of control strategies to overcome these potential FR performance issues.

In power systems, DC capacitors are widely used to simulate the inertial characteristics of the system [18]. Although the DC capacitor does not directly affect MPPT control, its stored electrostatic energy is relatively limited [19]. In order to further improve the FR performance of the system, in addition to the aforementioned FR schemes, energy storage technologies with fast responses can be introduced to achieve timely support and FR, including battery energy storage, superconducting energy storage, flywheel energy storage and supercapacitor energy storage, etc. [20,21]. However, the high investment cost will limit the large-scale practical applications of these energy storage technologies in power systems.

To overcome the problems of the FR control strategy mentioned above, this paper first introduces an equivalent linear model to describe the dynamic characteristics of FR increment power in droop control, aiming to gain a more comprehensive understanding of the behavior of the droop control system in FR. Secondly, based on this, an innovative improved decoupling FR strategy (IDFR) based on power tracking operation is further proposed. Considering that traditional FR strategies often use fixed coefficients to face variable disturbances and operational conditions that cannot meet the actual FR requirements, this paper takes frequency deviation (Δf) and df/dt as inputs and uses the fuzzy control method to determine the adaptive control coefficient. Finally, the FR adaptability and effectiveness of the IDFR strategy are verified under different operating conditions.

With the high proportion of new energy connected to the power grid resulting in a reduction in system inertia, it is imperative for new energy, mainly wind, to participate in frequency modulation. The strategy proposed in this paper weakens the “weakening effect” on the frequency support power caused by the interaction between the maximum power point tracking (MPPT) mode of a DFIG and its own speed in the traditional frequency modulation strategy. And fuzzy control is used to make DFIGs show excellent frequency modulation performance in the face of various disturbances and operating conditions, and maintain the frequency safety and stability of the system.

2. Control of DFIGs

Figure 1 shows a typical DFIG configuration with MPPT function, which mainly consists of basic components such as wind turbines, gearboxes, induction generators, and back-to-back rotor side converters (RSC) and grid side converters (GSC). Among them, the stator side is directly connected to the power grid, while the rotor side is connected to the power grid through a back-to-back converter. Specifically, RSC and GSC adopt typical vector control and PI control [22,23], where the main function of RSC is to achieve unit power factor operation. It adjusts the frequency and amplitude of the rotor voltage to

inject active power into the grid, aiming to ensure that the system can effectively achieve maximum power capture under different wind speeds and operating conditions, thereby improving the overall efficiency of the generator.

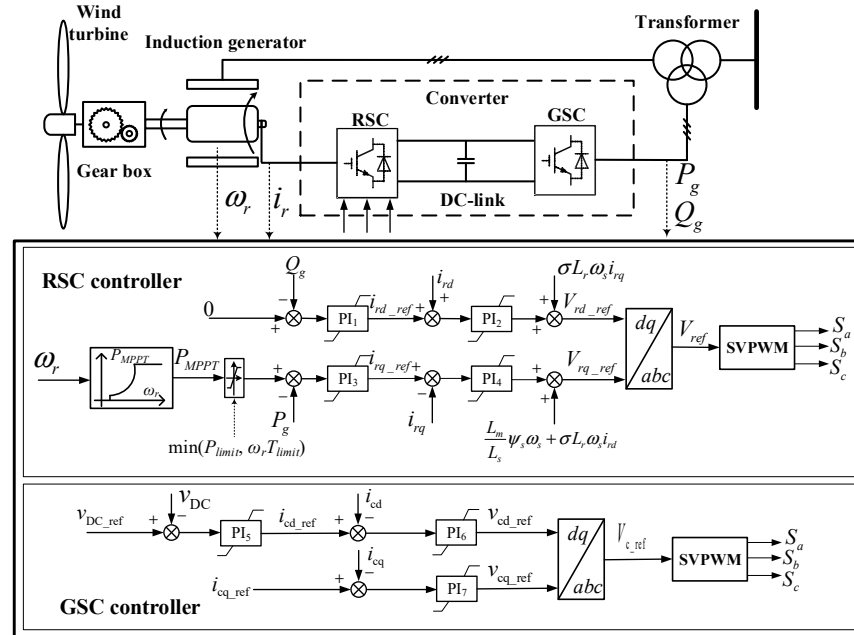


Figure 1. Typical structure of a DFIG.

The rotor current closed-loop control block diagram based on stator-flux-oriented vector control is shown in Figure 1. The control system includes two cascaded controllers: the outpower controller and the inner current controller. The feedback-measured active and reactive power are obtained from the generator output voltage and current. The references for active power and reactive power are compared with the feedback values [23]. The rotor current references for active and reactive power components are calculated after passing PI₁ and PI₃. Then, the rotor current for active and reactive power components is adjusted with the rotor current feedback values. The rotor voltage control command is obtained as in (1) by coupling with the feedforward compensation term and output of PI₂ and PI₄.

$$\begin{cases} u_{rd}^{\text{ref}} = \left[\left(k_{p1} + \frac{1}{s}k_{i1} \right) (Q_{\text{ref}} - Q) - i_{rd} \right] \left(k_{p2} + \frac{1}{s}k_{i2} \right) - \omega_s \sigma L_r i_{rq} \\ u_{rq}^{\text{ref}} = \left[\left(k_{p3} + \frac{1}{s}k_{i3} \right) (P_{\text{ref}} - P) - i_{rq} \right] \left(k_{p4} + \frac{1}{s}k_{i4} \right) + \omega_s \sigma L_r i_{rd} + \omega_s \frac{L_m}{L_s} \psi_s \end{cases} \quad (1)$$

where u_{rd}^{ref} and u_{rq}^{ref} are the rotor voltage references for dq -axis components, respectively; i_{rd} and i_{rq} are the rotor current command for dq -axis components; P_{ref} , Q_{ref} , P , and Q are the reference and measurements for active power and reactive power of DFIGs, respectively; k_{p1} , k_{i1} , k_{p2} , k_{i2} , k_{p3} , k_{i3} , k_{p4} , and k_{i4} , are the gains of PI₁, PI₂, PI₃, and PI₄, respectively; L_r , L_m , and L_s are rotor, stator, and magnetizing inductances, respectively; and ω_s , σ , and Ψ_s are the slip angular velocity, leakage factor, and flux linkage of stator, respectively.

The power characteristics of the DFIG running on MPPT are as follows:

$$P_{MPPT} = \frac{1}{2} \rho \pi R^2 c_{p, \max} \left(\frac{\omega_r R}{\lambda_{\text{opt}}} \right)^3 = k_g \omega_r^3 \quad (2)$$

where k_g and λ_{opt} are the coefficient and optimal tip-speed ratio, respectively.

The deloading operation, which reserves a certain amount of power depending on the command, has been widely employed for frequency regulation. To achieve the deloading operation, when modifying the setting of the control coefficient for power operation in Equation (2), operating point A moves to the deloading curves and is then stabilized at A₁

or A_2 with a dynamic state, as shown in the blue lines of Figure 2. This dynamic process can be used for providing fast frequency responses for storing redundant power from the grid or releasing power to the grid. This is the key idea for designing a decoupled frequency regulation scheme.

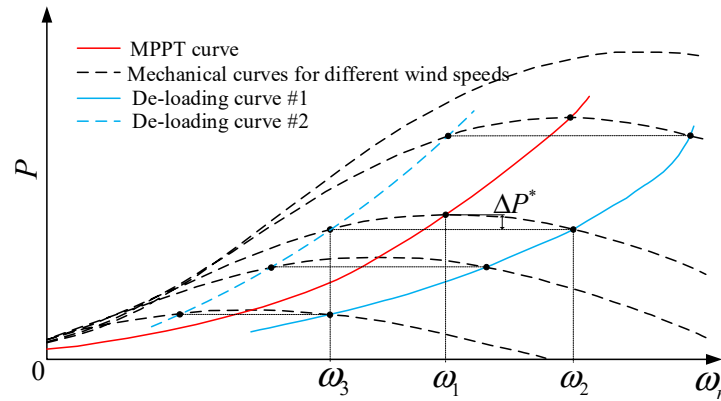


Figure 2. Operating characteristics of DFIGs.

3. Adaptive Frequency Regulation Scheme of DFIGs

Based on the deloading operation idea of frequency regulation, this section reveals the “weakening effect” in the traditional frequency modulation strategy, and proposes the variable power tracking control strategy of DFIGs based on fuzzy control.

3.1. Dynamic Characteristics of Frequency Regulation Incremental Power for Droop Control

Figure 3 shows the FR scheme of DFIGs with droop control. The power reference control loop consists of two parts: the output of the MPPT control loop (P_{MPPT}) and the output of the droop control (ΔP_{droop}).

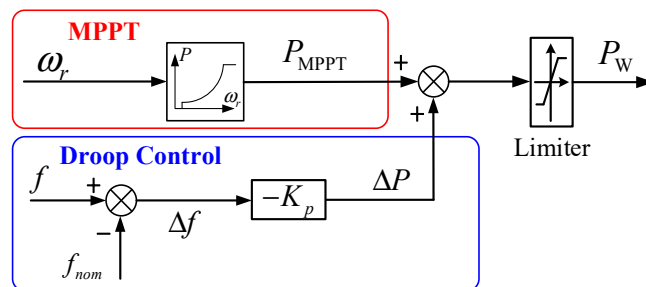


Figure 3. The droop control architecture of DFIGs.

In ref. [12], ΔP_{droop} can be expressed as

$$\Delta P_{droop} = -K_p(f - f_{nom}) = -K_p\Delta f \tag{3}$$

where K_p is the control gain representing droop control as an adjustment parameter that determines the degree of response of droop control to grid frequency offset, f is the actual frequency of the power grid, f_{nom} represents the expected operating frequency of the power grid, and Δf is the offset of the grid frequency, that is, the difference between the actual frequency and the reference frequency.

When a DFIG participates in FR through droop control, its rotor speed will decrease or increase according to the sign of Δf , which leads to the deviation of the DFIG from the MPPT operation curve. Therefore, changes in the MPPT control loop can be expressed in the following expressions:

$$\Delta P_{MPPT} = k_g(\omega_0 + \Delta\omega_r)^3 - k_g\omega_0^3 \approx -3k_g\omega_0^2\Delta\omega_r \tag{4}$$

where ΔP_{MPPT} is the power variation in the MPPT control loop, that is, the power change caused by the deviation of the DFIG from the MPPT, ω_0 is the DFIG initial speed, and $\Delta\omega_r$ is the rotor speed deviation, calculated by $\Delta\omega_r = \omega_r - \omega_0$.

According to Equation (4), the actual power injected by the DFIG into the power grid during FR is

$$\Delta P_{act} = \Delta P_{MPPT} + \Delta P = -3k_g\omega_0^2\Delta\omega_r + (-K_p\Delta f) \tag{5}$$

According to Figure 4 and Equation (5), it can be seen that after the disturbance arrives at time t_0 , as with the increase in Δf , an increase in ΔP and $\Delta\omega_r$ will be caused, which leads to the deviation of ΔP_{act} from the ideal power injected by the DFIG into the grid. The deviation in ΔP_{act} depends on the gain coefficient K_p of the droop control loop and the size of the disturbance.

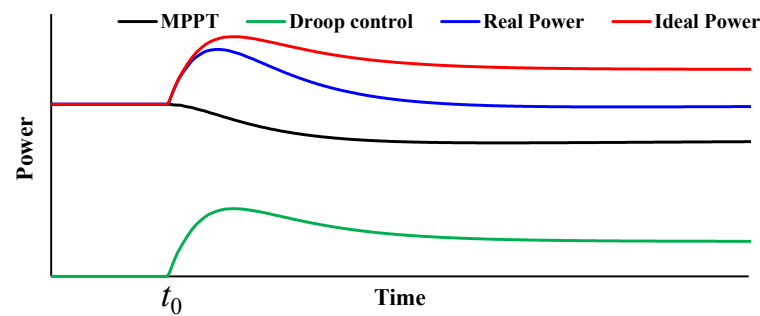


Figure 4. Power dynamic characteristics under droop control.

Figure 5 illustrates the incremental power to the power grid with different settings of K_p . Larger $\Delta\omega_r$ leads to ΔP_{MPPT} of a larger value so as to decrease the incremental power for frequency regulation, which will impair the contribution for improving the maximum frequency deviation. With a large setting of K_p , ΔP_{act} will be large, so as to release more kinetic energy to the power grid, but the risk of causing the shutdown of the DFIG will be increased, even causing an instability of the power system [19].

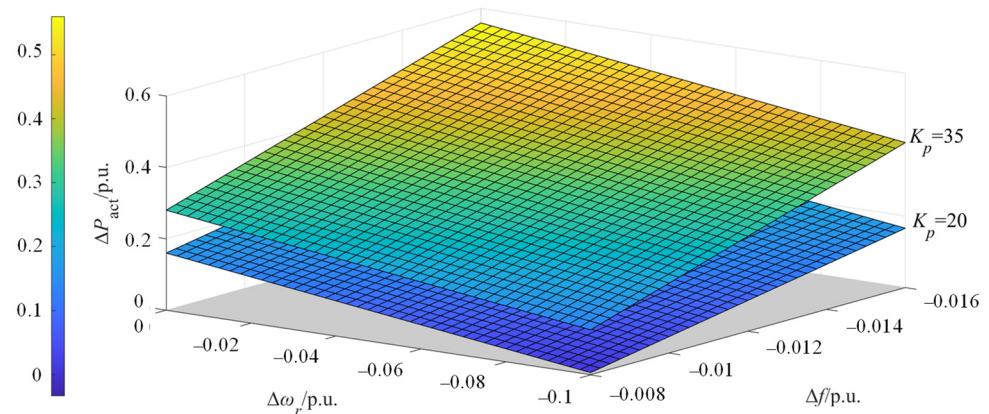


Figure 5. Incremental power with different K_p .

3.2. Proposed Frequency Regulation Scheme Based on Fuzzy Control

Based on the aforementioned analysis, difficulties arise when assigning the setting of K_p , and part of ΔP should compensate for ΔP_{MPPT} so as to decrease ΔP_{act} , thereby adversely impacting the performance for FR.

In this paper, direct control based on coefficient change is adopted, especially for the power tracking operation (k_{var}) in the power-speed controller, which is designed to realize the deviation of the DFIG from the MPPT operation curve and participate in the system FR, as follows:

$$P_W = k_{var}\omega_r^3 = k_g(1 + \Delta k) \times \omega_r^3 \tag{6}$$

where Δk is the coefficient for various power tracking operations of DFIG.

As in Equation (6), in the absence of disturbance, the DFIG operates in MPPT mode. However, when the system detects disturbances, due to the introduction of the coefficient of variation Δk , the DFIG will deviate from the MPPT working point to participate in FR, thus possessing dual FR capability. Specifically, this will happen when the grid $\Delta f < 0$, due to the implementation of positive Δk . The operating point of the DFIG will move to the left of the MPPT curve shown in Figure 6, and the trajectory changes will be represented from A \rightarrow B. In this case, DFIGs can more actively provide power to maintain the stability of the grid frequency when dealing with disturbances caused by reduced grid frequency. On the other hand, when dealing with grid over-frequency disturbances (see trajectory A \rightarrow C in Figure 6), due to the Δk being negative, the running point of the DFIG will move to the right, where ω_{\max} and ω_{\min} represent the maximum and minimum values in Figure 6, respectively. This FR response enables the DFIG to effectively absorb the energy of over-frequency and prevent any excessive power imbalance in the system.

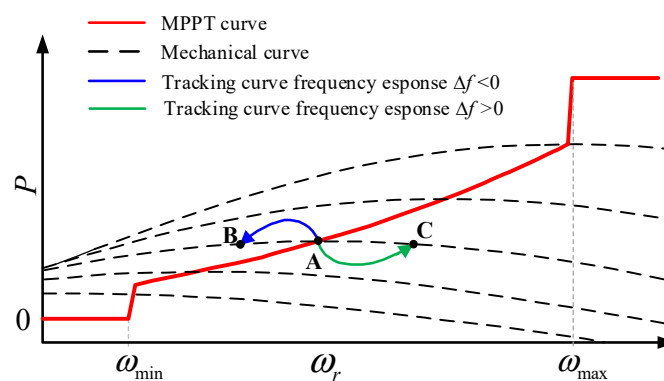


Figure 6. Proposed frequency regulation characteristics.

The amount of power released or absorbed by the DFIG depends on the setting of Δk : even if the use of the large fixed Δk could improve the frequency regulation capability, the stable operation of the DFIG will not be facilitated due to excessive rotor energy being released or absorbed, and over-compensation for frequency regulation will exist for a small frequency disturbance. On the other hand, if Δk is too small, the FR capability of DFIGs will not be able to meet the system requirements, and the FR potential will not be fully utilized, especially at high wind speeds.

A fuzzy controller is a kind of nonlinear controller that does not require the precise mathematical modeling of the controlled process and which has good robustness and adaptability [24]. Fuzzy control performs particularly practically, especially in situations where the controlled process is complex or it is difficult to establish an accurate mathematical model. Due to the difficulty in adapting to various disturbances and operating conditions with a fixed Δk setting, the setting of Δk becomes a comprehensive process. In this context, this paper proposes a frequency regulation scheme based on fuzzy control, where the input variables of the fuzzy controller are instantaneous Δf and df/dt . Specifically, the fuzzy control scheme enables DFIGs to dynamically adjust Δk based on instantaneous Δf and df/dt , and move according to the preset trajectory of Equation (6), making DFIGs more flexible in responding to grid disturbances and changes in operating conditions, and achieving more adaptive FR responses.

For the fuzzy controller, the variation ranges of Δf and df/dt are $[-0.8, 0.8]$ and $[-0.5, 0.5]$, respectively. In addition, to avoid the adverse impact of excessive Δk on frequency regulation, the adjustment range of Δk is set as $[-1.2, 1.2]$. To accurately reflect the control concept and avoid increasing the complexity of fuzzy inference rules, this paper divides the input and output fuzzy subsets into seven types, including NB (negative maximum), NM (negative moderation), NS (negative minimum), Z (zero), PS (positive minimum), PM (positive moderation), and PB (positive maximum). This classification helps to simplify the fuzzy logic reasoning system, making it easier to understand and implement.

Specifically, the fuzzy subsets of input and output are shown in Figure 7, while Table 1 illustrates the fuzzy logic rules used in this scheme, Considering the subjectivity of the membership function and fuzzy rule setting, it is still possible to improve this optimization in the future. These rules are used to derive the corresponding output under given input conditions. By dividing input and output into these seven types, the design of fuzzy control systems is more interpretable, making system operations more intuitive and clear.

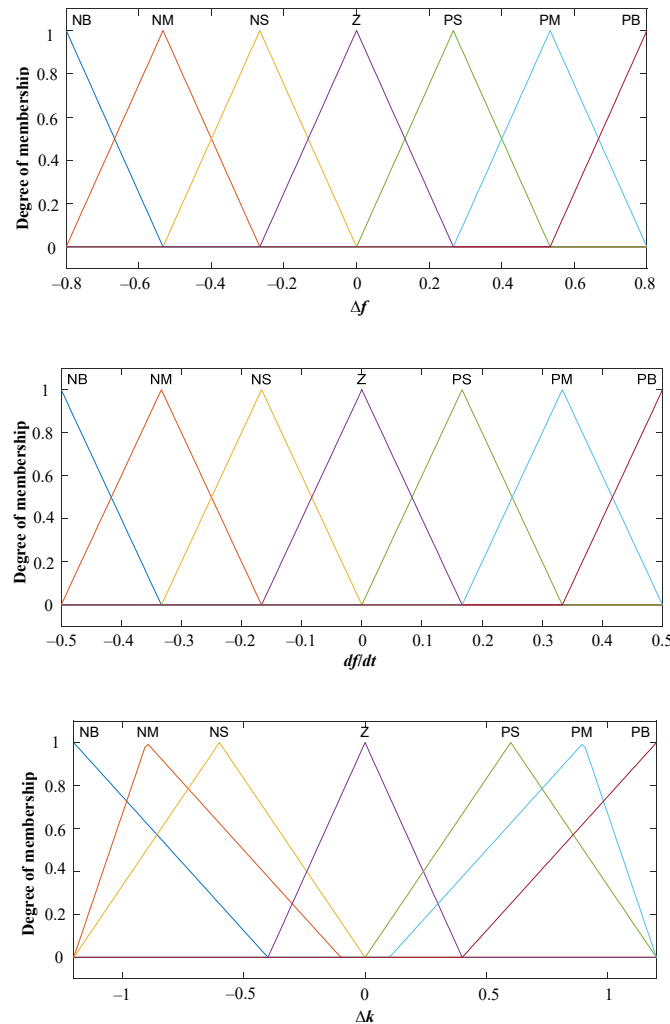


Figure 7. Membership function of fuzzy control.

Table 1. Fuzzy logic rules.

Δk	df/dt							
	NB	NM	NS	Z	PS	PM	PB	
Δf	NB	PB	PB	PB	PM	PS	PS	PM
	NM	PB	PB	PM	PM	PS	PS	PM
	NS	PB	PM	PM	PS	PS	PS	PS
	Z	PS	PS	Z	Z	Z	NS	NS
	PS	NS	NS	NS	NS	NM	NM	NB
	PM	NM	NS	NS	NM	NM	NB	NB
	PB	NM	NS	NS	NM	NB	NB	NB

The fuzzy inference principle in Table 1 is that Δf and df/dt have the same sign. When the system frequency is at the beginning stage of the frequency decrease, Δf is very small and df/dt is large. Therefore, Δk should be set to a larger value to prevent further frequency

decrease. When Δf is large and df/dt is small, this indicates that the grid frequency is gradually approaching the lowest point, and Δk can slightly decrease to avoid the excessive deceleration of the DFIG rotor kinetic energy release. In addition, before the lowest point of frequency, a large amount of power can be released to reduce the maximum frequency offset. When Δf and df/dt have different symbols, this indicates that Δf gradually decreases and df/dt gradually decreases to zero. In this case, to avoid the excessive deceleration of DFIGs, Δk needs to be reduced. This adjustment makes the system more flexible in adapting to changes in grid frequency, avoiding the problem of excessive deceleration. In summary, the output of fuzzy control based on Mamdani type was obtained, as shown in Figure 8.

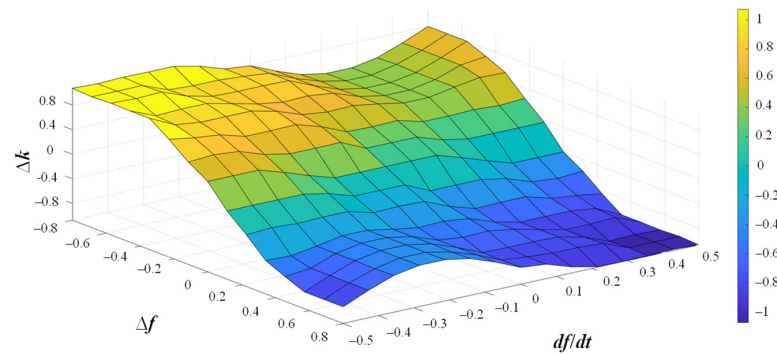


Figure 8. Results of fuzzy logic reasoning.

The flowchart of the IDFR strategy based on fuzzy control is shown in Figure 9. When Δf does not exceed the deadbands, the DFIG runs on the MPPT curve. When the disturbance occurs and Δf exceeds the deadbands, the DFIG detects its own operating state. If the DFIG speed is within its normal operating range ($0.7 < \omega_r < 1.25$), k_{var} changes according to Δf and df/dt , and the DFIG absorbs or releases the kinetic energy of the rotor to automatically participate in system frequency regulation due to the presence of Δk .

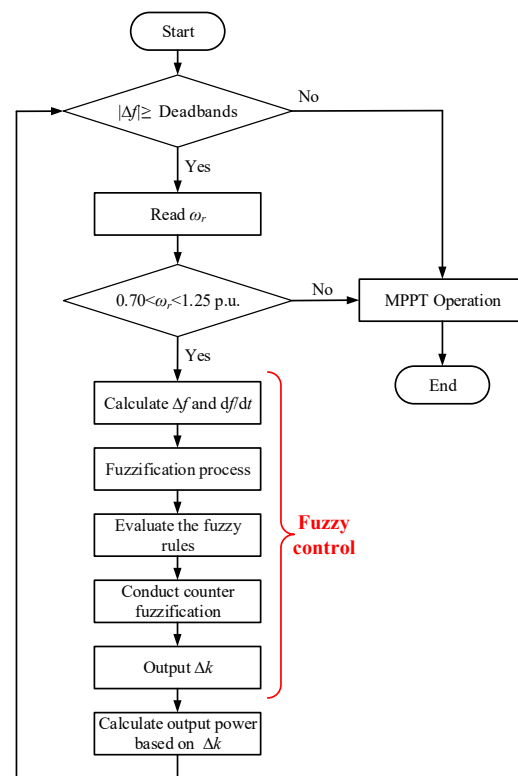


Figure 9. Control flowchart of the proposed scheme.

The proposed scheme in this article has the following characteristics: (1) By moving the operating curve of the DFIG, it achieves a fast frequency response without the need to measure wind speed and preset standby power, and provides the characteristic of dual regulation ability. This means that the system can quickly adapt to changes in grid frequency without the need to measure wind speed or set backup power in advance [25]. By adjusting Δk and moving the operation curve, the DFIG can flexibly participate in system frequency modulation to ensure frequency stability. (2) Under various disturbances and operating conditions, the power coefficient of the power tracking operation is determined by considering the fuzzy control of the df/dt and the instantaneous Δf . This fuzzy control solves the comprehensive problem of the distribution control coefficient, so that the system can adjust the power coefficient in real time according to the actual operation situation and the grid disturbance, and further enhances the adaptability of the system so that it can show good performance under different working conditions.

4. Model System and Simulation Results

To verify the effectiveness of the proposed IDFR scheme based on fuzzy control, this paper establishes a single-line model system on the EMTP-RV simulation platform. The system includes eight synchronous generators (TSG1-TSG8), a wind farm based on a DFIG, an asynchronous motor with a capacity of 350 MW, and a static load, as shown in Figure 10. The wind farm is formed by the aggregation of 24 DFIG units with a capacity of 5 MW [26], and the converters and mechanical subsystems of each DFIG are modeled according to Figure 1.

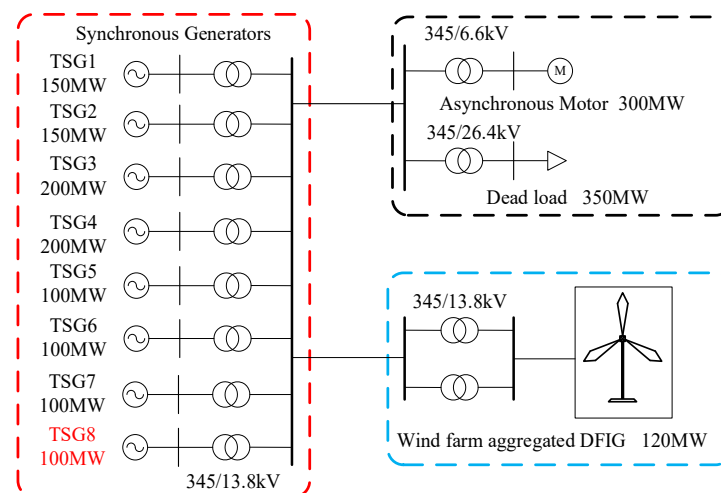


Figure 10. Power system model with a wind farm.

In this paper, the FR performance of the DFIG with MPPT, adaptive droop control [15], fixed control coefficient, and proposed dynamic control coefficient (Δk based on fuzzy control) under different wind conditions and disturbances are studied, as shown in Table 2. Among these factors, the K_p of droop control is set to 5% [16], and the frequency strategy of the fixed control coefficient is set to 0.5.

Table 2. Settings for the case studies.

	Size of Disturbance (MW)	Wind Speed (m/s)
Case 1	100	7.5
Case 2	100	9.0

4.1. Case 1: Wind Speed = 7.5 m/s, Disturbance = 100 MW

The simulation output results corresponding to various control strategies are shown in Figure 11 under a disturbance size of 100 MW. The increase in the power imbalance leads

to a decrease in the lowest frequency to 59.28 Hz. When the DFIG adopts adaptive droop control, the lowest frequency is 59.36 Hz, but the “weakening effect” of MPPT operation on the frequency support power results in a decrease in the actual output power of the DFIG by 0.02 p.u., as shown in Figure 11c. When the DFIG adopts a fixed Δk frequency regulation, the lowest point of the frequency increases to 59.38 Hz. The output power of FR is significantly increased compared to a fixed control coefficient, indicating that for severe disturbances to the system, as shown in Figure 11c, the power system requires more additional power to compensate for the power imbalance. Under the proposed method, the DFIG stall can be avoided, and the rotor kinetic energy can be maximized to supplement the system power shortage.

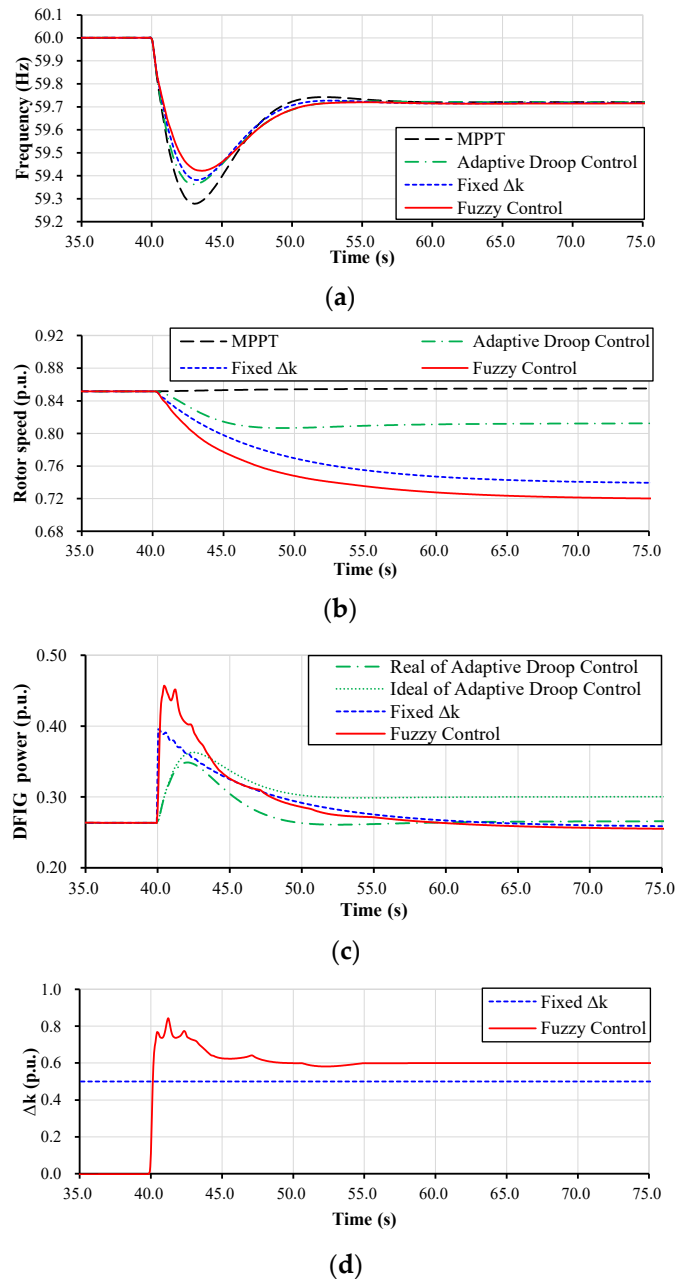


Figure 11. Results for Case 1. (a) System frequency. (b) Rotor speed. (c) The power of FR. (d) The value of Δk .

Due to the increase in the disturbance size, the maximum Δk increased by 0.16 p.u. When the DFIG adopts the frequency adjustment strategy proposed in this paper, the

kinetic energy released by the DFIG rotor increases by 0.08 p.u. (Figure 11b). Before the lowest frequency point, the lowest frequency point could be raised to 59.42 Hz, as shown in Figure 11a and Table 3. Due to the increase in disturbance, the minimum speed of the proposed scheme decreases to 0.72 p.u. Therefore, the DFIG releases more rotor kinetic energy to increase the lowest frequency point. Due to the fact that Δk can be modified to consider various interferences, it maintains excellent FR performance in improving the lowest frequency point, as shown in Figure 11d. This indicates that the proposed dynamic adjustment strategy can more flexibly respond to changes in system disturbances and maintain good performance under different operating conditions.

Table 3. Simulation results of Case 1.

	Frequency Lowest Point (Hz)	Minimum Rotative Speed (p.u.)	Maximum Output Power of a DFIG (p.u.)	The Difference between Ideal Power and Actual Power (p.u.)
MPPT	59.28	0.85	0.26	0
Adaptive droop control	59.36	0.80	0.34 (real)/0.36 (ideal)	0.02
Fixed Δk	59.38	0.74	0.40	0
Fuzzy control	59.42	0.72	0.46	0

4.2. Case 2: Wind Speed = 9.0 m/s, Disturbance = 100 MW

In this case, the wind speed increased to 9.0 m/s, resulting in higher rotor speed and more kinetic energy available for frequency modulation. Since the output power of the DFIG is calculated according to (6), even if the same Δk is used in the FR of fixed Δk , more power could be generated to support the dynamic frequency of the system (see Figure 12c), so that the lowest frequency increased to 59.45 Hz, which is more than that in Case 1 (see Figure 11a,c and Table 4). For the proposed dynamic Δk scheme, due to the increase in rotor speed, more power is injected into the grid, thereby increasing the lowest frequency to 59.49 Hz, as shown in Figure 12a,c.

Table 4. Simulation result of Case 2.

	Frequency Lowest Point (Hz)	Minimum Rotative Speed (p.u.)	Maximum Output Power of a DFIG (p.u.)	The Difference between Ideal Power and Actual Power (p.u.)
MPPT	59.28	1.02	0.46	0
Adaptive droop control	59.45	0.93	0.63 (real)/0.67 (ideal)	0.04
Fixed Δk	59.45	0.88	0.69	0
Fuzzy control	59.49	0.86	0.79	0

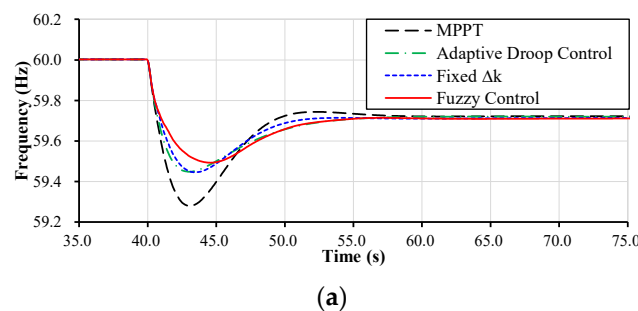


Figure 12. Cont.

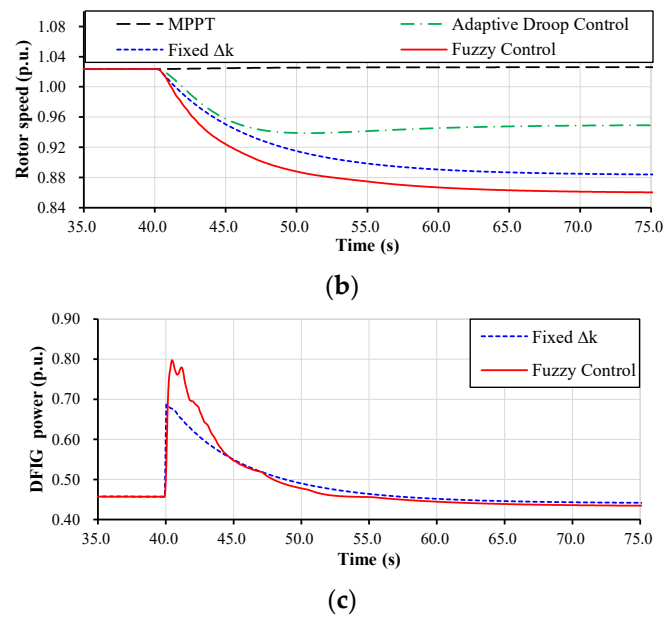


Figure 12. Results for Case 2. (a) Frequency. (b) Rotor speed. (c) The power of FR.

5. Conclusions

This research first introduces an equivalent linear model to describe the incremental power dynamic characteristics of an FR system with droop control. Secondly, an improved strategy for incremental power dynamics based on power tracking operation is proposed, namely the IDFR strategy, which aims to improve the frequency minimum point and df/dt of the system. Considering the problem of the insufficient adaptability of traditional fixed coefficient FR strategies in the face of various disturbances and operating conditions, this paper adopts a fuzzy control method, which adaptively determines the control coefficient of power tracking operation by considering Δf and df/dt as inputs. The proposed control scheme has the following significant advantages:

- (1) The power coefficient of the power tracking operation is effectively solved by introducing fuzzy control, which comprehensively considers the df/dt and Δf , thus effectively solving the comprehensive problem of control coefficient allocation. The application of fuzzy control enables the system to respond more flexibly to complex and changing working environments, improving the robustness and adaptability of the control.
- (2) The proposed IDFR strategy exhibits excellent performance in the face of various interferences and operating conditions. By effectively adjusting the control coefficient of the power tracking operation, the system can maintain the frequency's lowest point under different working conditions, and significantly improve the df/dt . This advantage makes the system more stable and responsive, with significantly enhanced adaptability.

At present, fuzzy control is used to make the fan adapt to different operating conditions. Considering the complexity and flexibility of fuzzy control, different parameter optimization methods will be constructed at a later stage to determine the key parameters of frequency modulation.

Author Contributions: X.X., J.H. and S.S. contributed to the conception and design of the proposed strategy. All authors wrote and edited the manuscript. All authors have read and agreed to the published version of the manuscript.

Funding: This work was supported by the National Natural Science Foundation of China (52307208) and the Nantong Science and Technology Plan Project (grant number JC12022071).

Data Availability Statement: Data are available upon request.

Conflicts of Interest: The authors declare no conflicts of interest.

References

1. Global Wind Energy Council. Global Wind Report 2020. 2021. Available online: <https://gwec.net/global-windreport-2021/#Download> (accessed on 2 March 2021).
2. Yang, D.; Li, J.; Jin, Z.; Yan, G.; Wang, X.; Ding, L.; Zhang, F.; Terzija, V. Sequential Frequency Regulation Strategy for DFIG and Battery Energy Storage System Considering Artificial Deadbands. *Int. J. Electr. Power Energy Syst.* **2024**, *155*, 109503. [CrossRef]
3. Yang, D.; Wang, X.; Chen, W.; Yan, G.G.; Jin, Z.; Jin, E.; Zheng, T. Adaptive Frequency Droop Feedback Control-Based Power Tracking Operation of a DFIG for Temporary Frequency Regulation. *IEEE Trans. Power Syst.* **2024**, *39*, 2682–2692. [CrossRef]
4. Lyu, X.; Jia, Y.; Dong, Z. Adaptive frequency responsive control for wind farm considering wake interaction. *J. Mod. Power Syst. Clean Energy* **2021**, *9*, 1066–1075. [CrossRef]
5. Miller, N.; Shao, M.; Venataraman, S. California ISO: Frequency Response Study. 2019. Available online: <http://www.uwig.org/Report-FrequencyResponseStudy.pdf> (accessed on 9 November 2019).
6. EirGrid; SONI. *Ensuring a Secure, Reliable and Efficient Power System in a Changing Environment*; Technic Report; EirGrid: Dublin, Ireland, 2011.
7. National Grid UK. *Grid Code Review Panel Paper, Future Frequency Response Services*; National Grid Group: London, UK, 2010.
8. GB/T 36994-2018; Wind Turbines-Test Procedure of Grid Adaptability. China Machinery Industry Federation: Beijing, China, 2018.
9. Nordic Grid Code 2007 (Nordic Collection of Rules). Nordel. 2007. Available online: <https://www.entsoe.eu/> (accessed on 10 November 2018).
10. Hydro Québec TransÉnergie. *Transmission Provider Technical Requirements for the Connection of Power Plants to the Hydro Québec Transmission System*; Hydro Québec TransÉnergie: Montréal, QC, Canada, 2009.
11. Zeni, L.; Rudolph, A.J.; Münster-Swendsen, J.; Margaritis, I.; Hansen, A.D.; Sørensen, P. Virtual inertia for variable speed wind turbines. *Wind. Energy* **2013**, *16*, 1225–1239. [CrossRef]
12. Yang, D.; Jin, Z.; Zheng, T.; Jin, E. An Adaptive Droop Control Strategy with Smooth Rotor Speed Recovery Capability for Doubly-fed Induction Generators. *Int. J. Electr. Power Energy Syst.* **2022**, *115*, 107532. [CrossRef]
13. Ye, H.; Pei, W.; Qi, Z. Analytical modeling of inertial and droop responses from a wind farm for short-term frequency regulation in power systems. *IEEE Trans. Power Syst.* **2016**, *31*, 3414–3423. [CrossRef]
14. Kheshti, M.; Lin, S.; Zhao, X.; Ding, L.; Yin, M.; Terzija, V. Gaussian Distribution-Based Inertial Control of Wind Turbine Generators for Fast Frequency Response in Low Inertia Systems. *IEEE Trans. Sustain. Energy* **2022**, *13*, 1641–1653. [CrossRef]
15. Hu, Y.-L.; Wu, Y.-K. Approximation to frequency control capability of a DFIG-based wind farm using a simple linear gain droop control. *IEEE Trans. Ind. Appl.* **2019**, *55*, 2300–2309. [CrossRef]
16. Lee, J.; Jang, G.; Muljadi, E.; Blaabjerg, F.; Chen, Z.; Kang, Y.C. Stable short-term frequency support using adaptive gains for a DFIG-based wind power plant. *IEEE Trans. Energy Convers.* **2016**, *31*, 1068–1079. [CrossRef]
17. Jiang, Q.; Zeng, X.; Li, B.; Wang, S.; Liu, T.; Chen, Z.; Wang, T.; Zhang, M. Time-Sharing Frequency Coordinated Control Strategy for PMSG-Based Wind Turbine. *IEEE J. Emerg. Sel. Top. Circuits Syst.* **2022**, *12*, 268–278. [CrossRef]
18. Zeng, X.; Liu, T.; Wang, S.; Dong, Y.; Chen, Z. Comprehensive coordinated control strategy of PMSG-based wind turbine for providing frequency regulation services. *IEEE Access* **2019**, *7*, 63944–63953. [CrossRef]
19. Li, Y.; Xu, Z.; Wong, K.P. Advanced control strategies of PMSG-based wind turbines for system inertia support. *IEEE Trans. Power Syst.* **2017**, *32*, 3027–3037. [CrossRef]
20. Zhao, H.; Wu, Q.; Hu, S.; Xu, H.; Rasmussen, C.N. Review of Energy Storage System for Wind Power Integration Support. *Appl. Energy* **2015**, *137*, 545–553. [CrossRef]
21. Bao, W.; Wu, Q.; Ding, L.; Huang, S.; Terzija, V. A hierarchical inertial control scheme for multiple wind farms with BESSs based on ADMM. *IEEE Trans. Sustain. Energy* **2021**, *12*, 1461–1472. [CrossRef]
22. Fernandez, L.M.; Garcia, C.A.; Jurado, F. Comparative study on the performance of control systems for doubly fed induction generator wind turbines operating with power regulation. *Energy* **2008**, *33*, 1438–1452. [CrossRef]
23. Petersson, A. *Analysis Modeling and Control of Doubly-Fed Induction Generators for Wind Turbines*; Chalmers Tekniska Hogskola: Göteborg, Sweden, 2005.
24. Ying, H. Constructing nonlinear variable gain controllers via the Taka-gieSugeno fuzzy control. *IEEE Trans. Fuzzy Syst.* **1998**, *2*, 226–234. [CrossRef]
25. Bian, X.; Zhang, J.; Ding, Y.; Zhao, J.; Zhou, Q.; Lin, S. Microgrid frequency regulation involving low-wind-speed wind turbine generators based on deep belief network. *IET Gener. Transm. Distrib.* **2020**, *14*, 2046–2054. [CrossRef]
26. Zhang, X.; Zhang, Y.; Fang, R.; Xu, D. Impedance Modeling and SSR Analysis of DFIG Using Complex Vector Theory. *IEEE Access* **2019**, *7*, 155860–155870. [CrossRef]

Disclaimer/Publisher’s Note: The statements, opinions and data contained in all publications are solely those of the individual author(s) and contributor(s) and not of MDPI and/or the editor(s). MDPI and/or the editor(s) disclaim responsibility for any injury to people or property resulting from any ideas, methods, instructions or products referred to in the content.